DIRECT OBSERVATION OF THE TUMBLING OF OSB STRANDS IN AN INDUSTRIAL SCALE COIL BLENDER

Gregory D. Smith†

Assistant Professor
Department of Wood Science
The University of British Columbia
2935–2424 Main Mall
Vancouver, BC
Canada V6T 1Z4

ABSTRACT

A series of experiments were carried out in an 11- by 35-ft industrial scale rotary drum blender in which a small amount of OSB furnish was placed, and the motions of strands were recorded with a video camera at various drum rotation speeds. As the blender rotated, the strands were lifted up by the flights—short fins inside and running the length of the blender—until they sloughed off and fell to the bottom of the drum. At low rotation speeds, the strands fell a short distance as they sloughed from flight to flight; at intermediate speeds, the strands fell across the diameter of the drum; and at higher speeds the freefall distance decreased again and was similar to the low speed case. The distance through which the strands fell with each revolution was shown theoretically to be inversely proportional to drum speed. The residence time of the stands in the blender set at a tilt angle of 3° was measured for five drum speeds and found to be directly proportional to drum speed. It was concluded that the speed that produces the most uniform dispersion of resin on the strands is a compromise between that which is high enough to ensure that the strands will slough from the flights many times, but low enough to provide sufficient time for the strand to twirl and flip and become coated with resin. The potential advantages of using specially shaped atomizer booms to direct strand flow to maximize the uniformity of the resin dispersion over the strand surface is also discussed.

Keywords: Blending, strand tumbling, furnish curtain, composites, OSB.

INTRODUCTION

The blending of strands with resin for the production of OSB occurs almost exclusively in rotary drum blenders. The objective of blending is to coat wood strands with resin and wax to produce a strong and dimensionally stable board. When required, biocides can also be incorporated to produce a more durable composite board. There are few reports in the literature on the effect of blender operating parameters on board properties, although there has been some work on the effect of resin spot size dispersion on the mechanical properties of OSB. Work by Carroll and McVey (1962), Lehmann (1965), Christensen and Robitschek (1974), and Kamke et al. (1996a), reported that properties of boards are enhanced by a finely dispersed and evenly distributed resin. Research to quantify resin coverage on strands has also been undertaken (Kamke et al. 1996a and b; Saunders and Kamke 1996), but researchers have not attempted to relate their findings to the operational parameters of the blender. Indeed little is known about the behavior of strands inside OSB blenders.

An industrial OSB blender consists of a large rotating drum fitted with infeed and exit chutes. The size of the drum ranges from 20 ft in length by 8 ft in diameter (Beattie 1984; Coil and Kasper 1984; and Lin 1984) up to 45 ft in length by 11 ft in diameter (Coil 2003a). The rotational axis of the drum is inclined, or tilted, between 1 to 6 degrees to the horizontal. Flights are fitted inside the blender to facilitate tumbling and strand separation. These are short fins running the length of the drum, usually 5 to 6 in. high, mounted on, and equally spaced around, the interior circumference of the drum. Drum rotation

†Member of SWST.

speeds vary depending on the type of resin being applied to the strands. For the case of an 11-ft diameter blender using powdered PF-resin, the drum rotates between 6 to 12 rpm; for a liquid PF-resin faster rotation is required, between 16 to 23 rpm. The actual rotation speed used will depend on the blending strategies employed in a plant and on the height and shape of the flights installed in the blender; thus the actual drum speed used may differ somewhat from these values (Coil 2003a).

A picture of a commercial blender is shown in Fig. 1. The flow of the center of a mass of strands through a blender is shown schematically in Fig. 2 by the dotted lines. Strands enter
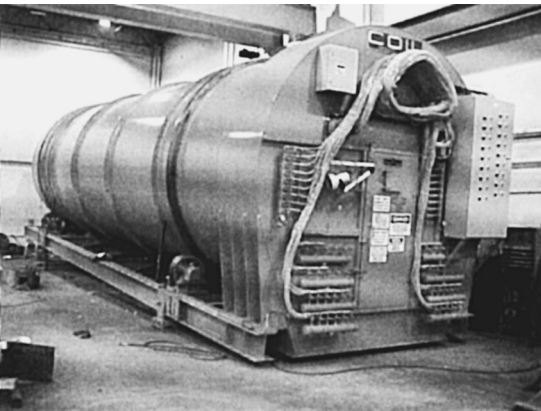
the blender through the infeed chute at the high end of the drum and are lifted up by the flights as the drum rotates. Strands eventually slough off the flights at detachment angle α and fall to the bottom of the drum following a turbulent path that is approximately parabolic. This process is repeated several times with the inclination of the drum steadily moving the strands along the length of the drum towards the exit chute. As they tumble, the strands are exposed to a fine mist of resin dispersed by atomizers located on a boom or booms running the length of the blender.

The stream of strands sloughing off the flights has been referred to by Coil and Kasper (1984) as a *furnish curtain.* They noted that the position of this curtain across the width of the blender can be changed by adjusting the drum rotation speed; strands will slough from flight to flight at very low speed, fall the diameter of the drum at intermediate speed, and centrifuge at high speed. Coil and Kasper (1984) photographed strands tumbling in a 20-ft-long by 8-ft-diameter blender rotating at 18 rpm; but it is difficult to determine the pattern of strand flow from their figure. The motion of the strands inside a blender can be more easily seen in a photograph from Beattie (1984) of strands tumbling inside a running labscale blender where the blender door was removed.

Apart from these reports, there are no other published studies on the motion of strands inside

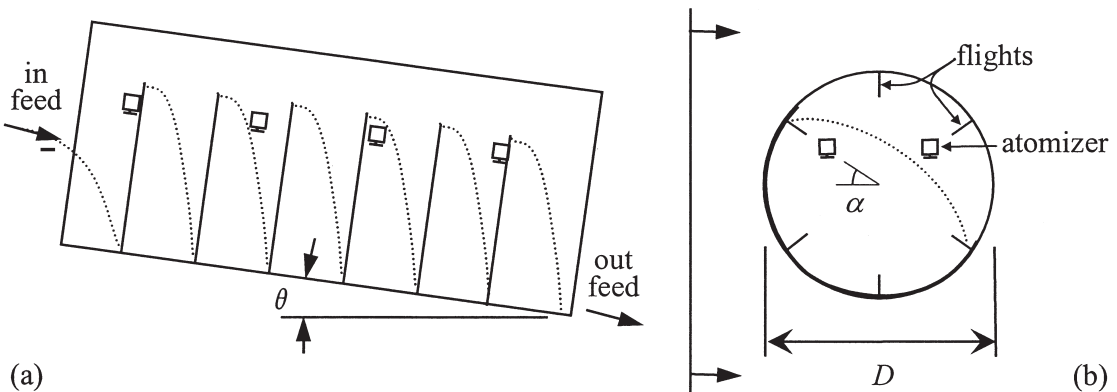FIG. 1. The Coil 11-ft by 35-ft rotary drum blender.

FIG. 2. The motion of the center of mass of a strand bundle through a blender: (a) side view and (b) view looking along axis of rotation.

OSB blenders. This study examines the motion of strands inside a large, industrial-scale blender. The aim is twofold: first, to more precisely examine the effect of rotation speed on strand tumbling and residence time; and second, to discuss the implication of these observations for the commercial blending and manufacture of OSB.

THEORY

As the motion of wood strands in a blender is complex, it is useful to review the forces acting on loose piles of material and on bodies rotating in uniform circular motion. Any loose material such as sand or wood chips will form a conical pile when poured on to a flat surface, as shown in Fig. 3. The angle formed between the outer surface of the cone and the horizontal is referred to as the angle of repose φ and is a measure of the internal friction within the material. If the coefficient of friction between adjacent particles is low, φ will be small; if the friction between particles is high, φ will be large.

The forces acting on a strand or strand bundle will depend on its position within the blender. These forces are similar to those acting on the charge in a ball mill, and the theory developed here draws on the foundation work of Davis (1919). For those strands in contact with the drum liner or a flight, the motion of strands will be controlled by a combination of gravitational and centripetal forces and the frictional forces between the strands and the liner. Assuming (1) the strands move as a coherent block rather than as individual pieces and (2) the strand or strand bundle is in contact with the drum liner, the following three equations can be used to describe the forces acting on strands inside a blender. The gravitational force is given by:
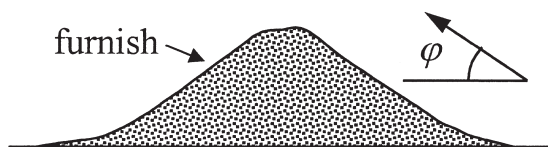
$$F_g = mg, \tag{1}$$

where m is the mass of the strand or strand bundle and g the acceleration due to gravity. The centripetal force due to the rotation of the blender is given by:

$$F_\omega = m\omega^2 R, \tag{2}$$

where ω is the rotational speed (angular velocity) of the blender drum and R the distance from the drum axis. The frictional force is given by:

$$F_f = \mu F_n, \tag{3}$$

where μ is the coefficient of friction between the strand surface and the drum wall and F_n is the normal force exerted by the strand or strand bundle on the drum liner due to gravitational and centripetal forces.

Detachment angle

The detachment angle, α, at which a strand bundle begins to fall away from the drum liner, shown in Fig. 2, is determined by the balance of gravitational and centripetal forces acting on it. Discounting friction between the strands and the flight, the strands will begin to slough once the gravitational force exceeds the centrifugal force. Setting Eq. (1) equal to Eq. (2) and simplifying produces:

$$\alpha = \text{Arccos}\left(\frac{R\omega^2}{g}\right) \tag{4}$$

Thus, α increases with angular velocity ω and distance R from the drum axis. This equation is valid for the case where the strands are in constant contact with the drum liner and not sliding over it. As will be discussed later, this R dependence produces a range of detachment angles as the strand farthest from the drum liner is the first to detach and fall.

Model development

Strand motion at low speed.—The angle of detachment also affects the distance through which the strands fall. In the case of a blender drum rotating very slowly, the contribution of the angular speed to the horizontal velocity of the strands

Fig. 3. Loose furnish pile showing the angle of repose.

will be negligible and the strands will slough off the flight and land on the flight immediately beneath it as shown schematically in Fig. 4a. Neglecting the curvature of the drum, the distance the strands fall, h, is approximately equal to the spacing between flights, i.e.,

$$h = \frac{\pi D}{n} \qquad (5)$$

where D is the diameter of the blender drum and n is the number of equally spaced flights around the circumference of the drum.

Since the axis of the blender is inclined to the horizontal by the tilt angle θ, the strands actually fall distance, d, and move an incremental distance, l, closer to the exit chute with each slough, shown schematically in Fig. 5. The incremental distance l is related to length the strands fall d as

$$l = d \sin \theta, \qquad (6)$$

or in terms of the distance perpendicular to the axis of rotation,

$$l = h \tan \theta. \qquad (7)$$

During one revolution the strands will slough from flight to flight n times and move towards the exit chute a distance of nl. Substituting Eq. (5) into Eq. (7), the total distance that the strands travel parallel to the drum axis at low drum speeds for one revolution l_{total}^{low}, can be expressed as:

$$l_{total}^{low} = nl = \pi D \tan \theta. \qquad (8)$$

Strand motion at intermediate speed.—Next consider the case where the drum is rotating at an intermediate speed where the total distance the strands fall will be maximum and approximately equal to the drum diameter D, as shown in Fig. 4b. The total distance the strands move toward the exit chute with each revolution, l_{total}^{int}, and can be obtained by substituting D for h in Eq. (7) to give:

$$l_{total}^{int} = D \tan \theta. \qquad (9)$$

Strand motion at high speed.—Finally, consider the case where the drum is rotating at high speed where the strands are almost pinned to the drum liner. If the drum is rotating fast enough, the detachment angle will become very large and the strands will begin to fall away from the flight
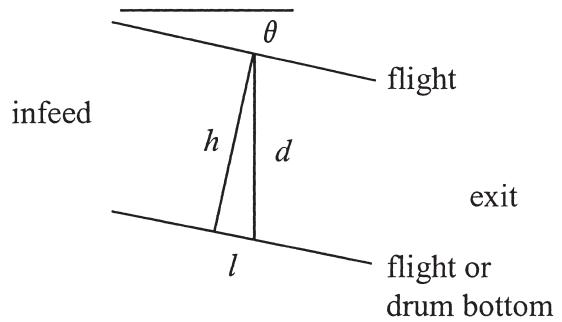

FIG. 5.   A schematic of the length l that the strands move along the length of the blender after sloughing off a flight and falling distance d to the bottom of the blender drum.
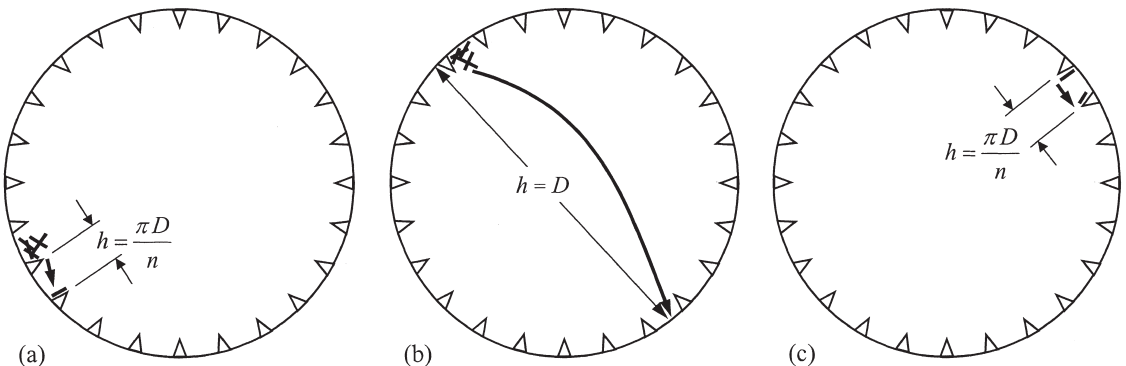

FIG. 4.   Comparison of the distance that strands fall in the blender when rotating at (a) low speed, (b) intermediate speed, and (c) high speed.

only to slide over the drum liner and land on the adjacent face of the next flight as shown in Fig. 4c. As was the case at low drum speeds, the distance h that the strands fall is approximately equal to the distance between the flights, i.e., $\pi D/n$. The key difference between this case and the low speed case is that the strands slide over the drum liner only once per revolution, and the total distance the strands move towards the exit chute is given by dividing Eq. (8) by n,

$$l_{total}^{high} = \frac{\pi D}{n}\tan\theta \tag{10}$$

Comparison of Eqs. (8)–(10) shows that the ratio of the incremental distance travelled towards the exit chute from low to intermediate to high rotation speeds is $\pi: 1 :\pi/n$. In other words, the distance the strands move parallel to the drum axis per revolution is inversely proportional to rotation speed. It is not clear from the above model whether residence time is directly proportional to drum speed for a given tilt angle and a means of coupling the distance travelled through the drum with the time required for the free fall of the strands is needed.

MATERIALS AND METHODS

The strands used in this work were mill-run strands supplied by the Ainsworth OSB plant in 100 Mile House, BC, Canada. Average strand dimensions and their associated 95% confidence intervals were 107 ± 7 mm in length by 16 ± 5 mm in width and 0.83 ± 0.13 mm in thickness. The average dimensions of the strands were determined by selecting ten strands at random and measuring their length and width to ± 1 mm and their thickness to ± 0.025 mm using digital callipers. Five sets of strands were prepared: each set consisted of two bags with a total mass of 33 kg and a bulk volume of approximately 0.53 m^3.

The industrial blender used in this work was an 11-ft diameter by 35-ft long blender made by Coil Manufacturing of Surrey, British Columbia, and fitted with 24–6 in. high UHMW polyethylene bull-nosed flights equally spaced around the interior circumference of the drum. The tilt angle, θ, of the blender was kept constant at 3°.

The interior of the blender was illuminated by five 500 watt halogen lights. The tumbling of the strands was recorded using a video camera with its optical axis aligned with the axis of rotation of the blender. The positions of the lights and camera are shown schematically in Fig. 6. The motion of strands was recorded at drum speeds of 12.5, 15.4, 18.2, 21.0, and 23.8 rpm. These experiments were run by setting the blender to the required rotation speed, turning on the video camera, verifying the drum speed, feeding the bags of strands into the blender, and recording their motion until the majority of the strands exited the blender through the exit chute.

The video tape of each experiment was digitized and converted into an mpeg movie file. Representative images of the strand tumbling patterns for each drum speed were obtained by extracting a single image from the mpeg movie using Adobe Premiere version 6.5; still images were obtained after approximately 3 drum revolutions and after the strand charge had advanced approximately three quarters of the length of the blender at the moment when the strands began to leave the field of view of the video camera.

RESULTS AND DISCUSSION

Representative images of the strand patterns in the blender for the different drum speeds after 3 revolutions and at the longer tumbling times are shown in Fig. 7 in which the drum is rotating clockwise.

As the strands were loaded into the blender, they fell to the bottom of the drum and were scooped-up by the flights. As the blender rotated, the strands on the top, outer surface of the bun-
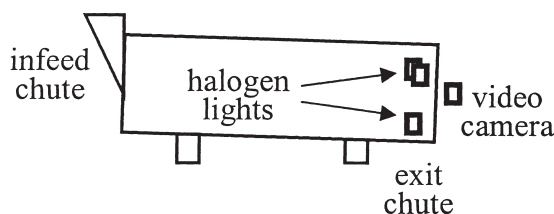

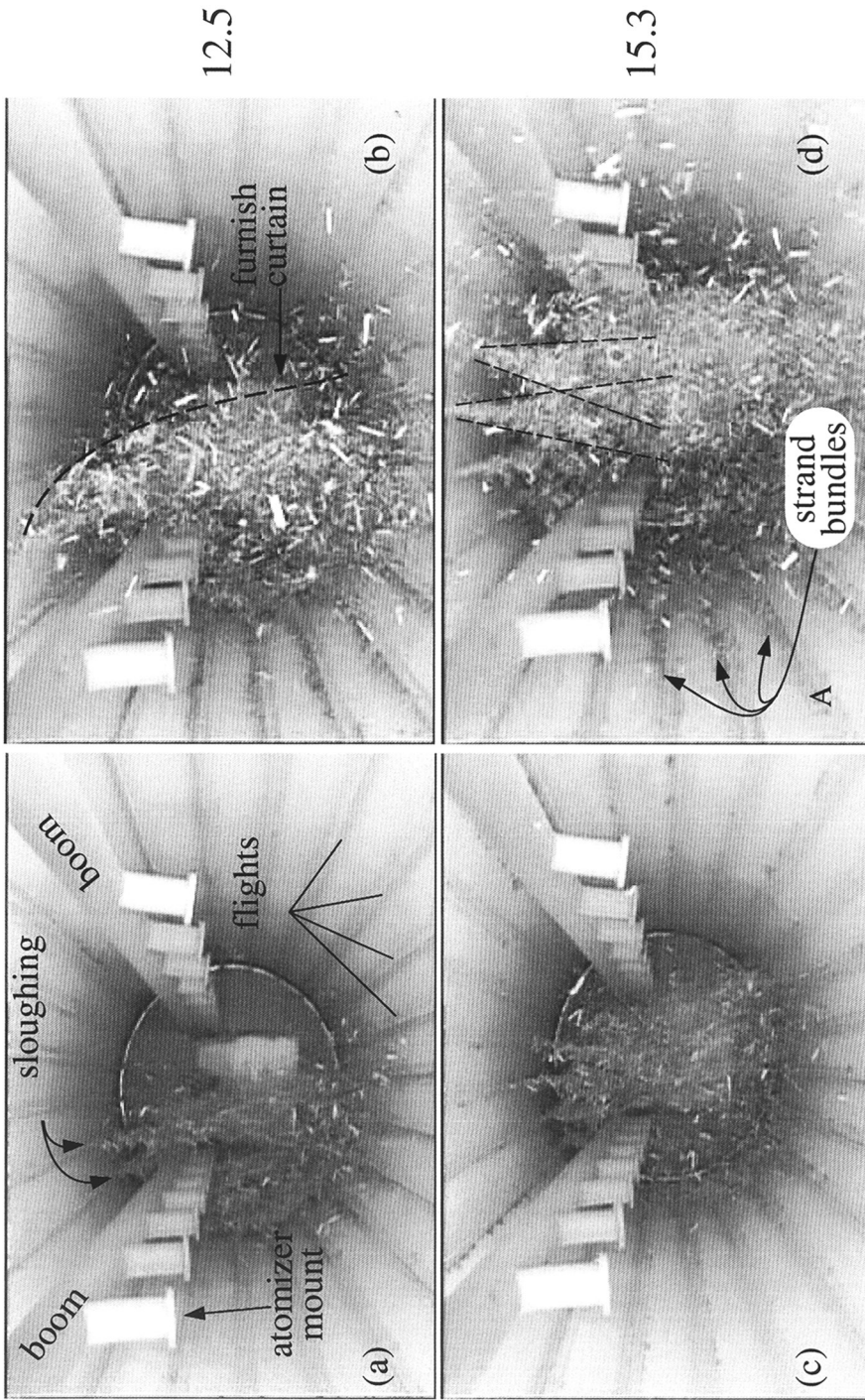FIG. 6. Position of the halogen lights and video camera in the blender.

FIG. 7a-d. Comparison of the tumbling behavior for different drum speeds. The images on the left side of the figure are taken after 3 revolutions and those of the right after the strands have travelled about three-quarters of the length of the drum (the number of revolutions are listed in Table 1). The rotation speeds are listed on the right side of the figure in rpm. Drum tilt angle is 3°.

FIG. 7e-h.   Comparison of the tumbling behavior for different drum speeds. The images on the left side of the figure are taken after 3 revolutions and those of the right after the strands have travelled about three-quarters of the length of the drum (the number of revolutions are listed in Table 1). The rotation speeds are listed on the right side of the figure in rpm. Drum tilt angle is 3°.
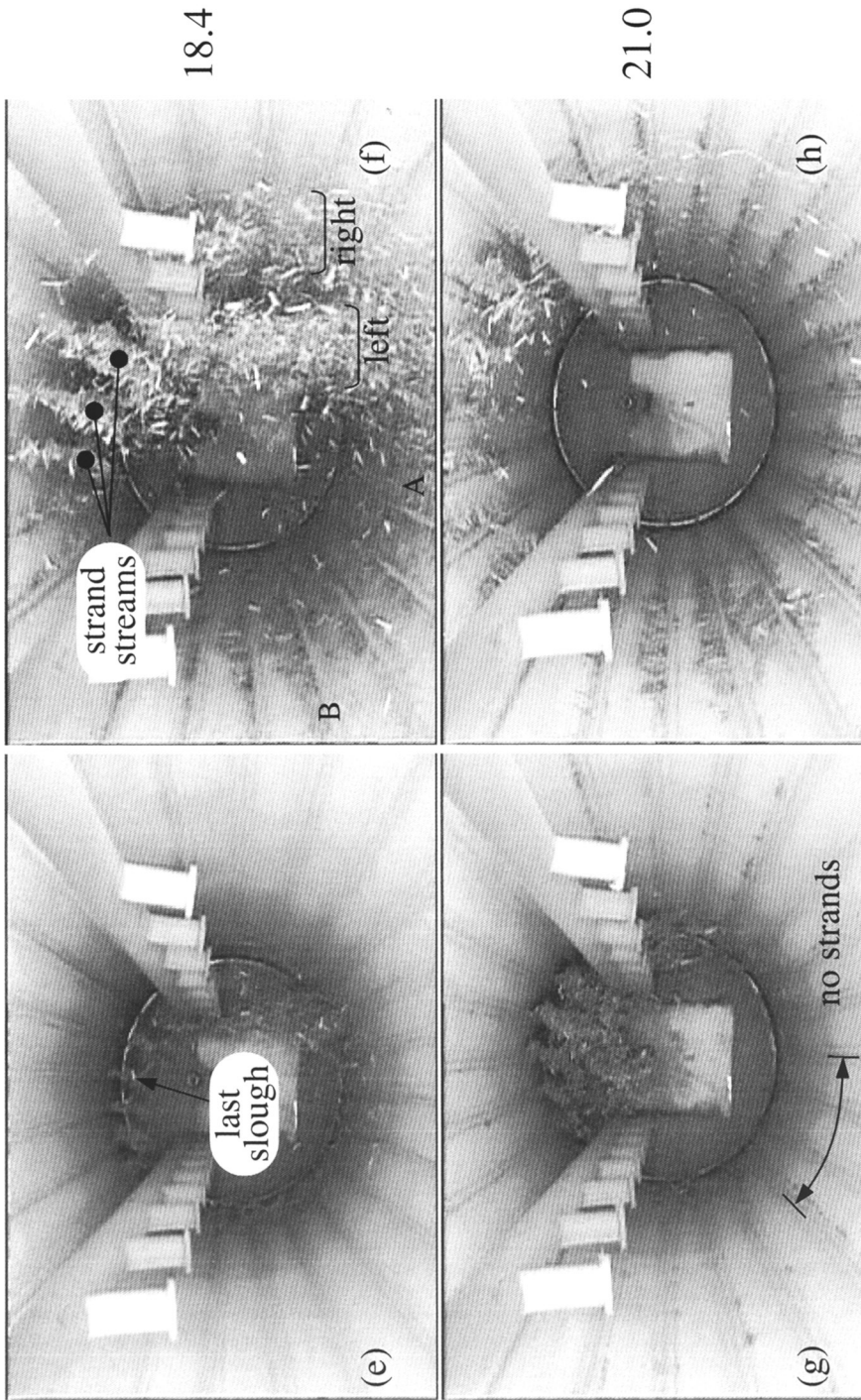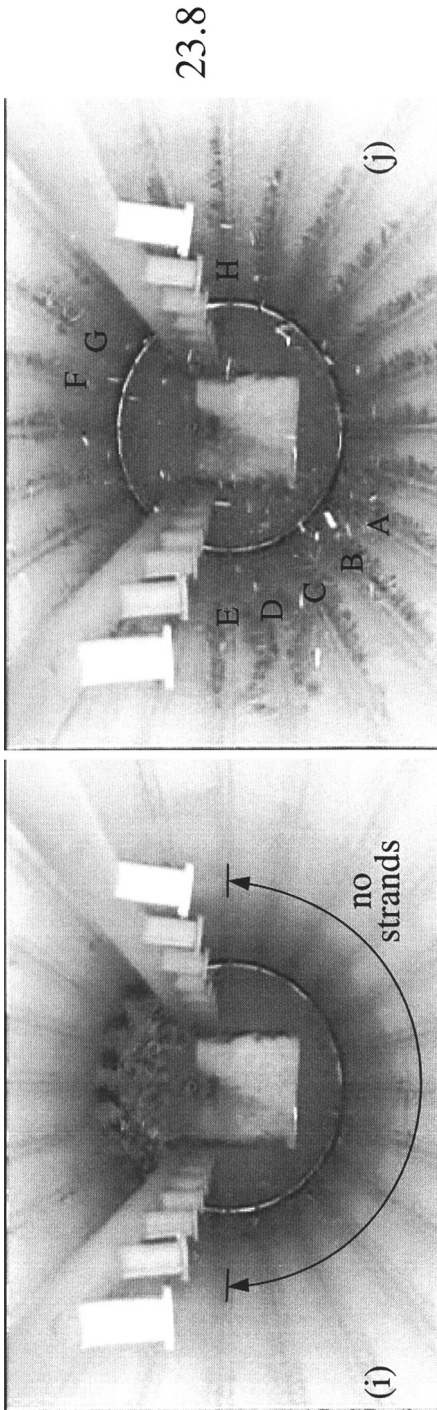
FIG. 7i-j.   Comparison of the tumbling behavior for different drum speeds. The images on the left side of the figure are taken after 3 revolutions and those of the right after the strands have travelled about three-quarters of the length of the drum (the number of revolutions are listed in Table 1). The rotation speeds are listed on the right side of the figure in rpm. Drum tilt angle is 3°.

dle reached the angle of repose and then slid off. Strands continued to slough off the bundle producing a continuous stream of strands until the frictional force between the bundle and the flight became lower than the frictional force between strands, at which point the whole bundle slid off the flight and fell to the bottom of the drum following what appears to be a parabolic path. At rotation speeds of 12.5, 15.3, and 18.4 rpm, some of the strands landed on the atomizer booms, slid off, and recommenced tumbling.

Adding the two bags of strands for each set to the blender sequentially made it difficult to compare the strand flow during the first few revolutions. There was always a 4- to 5- s lapse between pouring the first bag into the blender and pouring the second bag. For the 12.5 and 23.8 rpm rotation speeds, this meant that the second bag of strands landed in approximately the same position as the first bag. At the intermediate drum speeds, the second bag of strands did not land in the same place as the first bag, and this generally reduced the amount of time needed for the strands to distribute themselves around the circumference of the blender.

Effect of rotation speed on strand motion

At 12.5 rpm, shown in Figs. 7a and b, the strands were lifted up by the flights, sloughed off the flights, and fell to the floor of the blender forming a furnish curtain similar to that described by Coil and Kasper (1984). The shape of the front face of the furnish curtain is indicated in Fig. 7b by the dashed line and is approximately parabolic. The furnish curtain is the result of strands continuously sloughing off of the flights as the blender rotates and whose detachment angle is determined by rotation speed and distance from the drum axis (recall Eq. (4)) The centrifugal force exerted on a strand will depend on its position within the strand bundle (i.e., rotation radius). Strands closest to the drum liner experience the most centrifugal force, while the inner strands on the top of the bundle and farthest from the drum liner experience the least. Thus, as the drum rotates, the innermost strand on the top of the bundle will detach first. As the

drum rotates further, an angle will be reached where the centrifugal force acting on the next strand becomes less than the gravitational force and that strand will then fall. If there are many strands within the bundle, one would expect to see a steady stream of strands sloughing off the flights and falling to the bottom of the drum. The position where the strands began to slough off the flights is hidden by the left atomizer boom in Fig. 7a, but strands are easily seen sloughing from the two flights just to the right of this boom. Note that some of the strands from the first flight collided with the left atomizer boom as they fell. As the strands tumbled to the floor of the blender, it was observed that the predominant motion of the strands was rotation about their long axis (for convenience this will be referred to as "twirling") and occasionally rotation about their short axis (referred to as "flipping").

Increasing the drum speed from 12.5 to 15.3 rpm increased the centrifugal force the strands exerted on the drum liner. This increased the angle through which the blender must rotate before the strands slough off the flights. All strand motions observed for the 12.5 rpm blender speed also occurred at 15.3 rpm. Examination of Fig. 7c shows strands sloughing off from the flights between 10:30 and 12:00 o'clock, whereas at 12.5 rpm the sloughing occurred between 10:30 and 11:00 o'clock (Fig. 7a). As a strand bundle fell, it fanned out into a triangular shape (Fig. 7d), suggesting that the spread increases linearly with the distance fallen. Examination of those strands which fell from the third and fourth flights to the right of the left boom in Fig. 7d, indicated by the dashed lines, shows that the strands had mixed together at approximately the mid-point of the blender. The strand bundles also spread along their length, parallel to the axis of the drum, although this cannot be seen in the figure. It should be noted that this behavior is a result of the very small strand mass used in this work and is unlikely to occur in an industrial blender during normal operation because the strand mass at any point along the length of the blender will be approximately constant. This means that strands at a given position within the blender will be prevented from spreading length-

wise by the presence of other strands in front of and behind them. The motion of strands between flights near the bottom of the blender can also be seen in Fig. 7d. As the drum rotated, the strands between the flights slipped towards the lower flight to form strand bundles at the base of the flight.

Increasing the drum speed to 18.4 rpm (Figs. 7e and f) shifted the range of angles at which the strands sloughed off the flights. In Fig. 7e, strands sloughed off the first four flights just to the right of the left atomizer boom. The increase in speed means that the onset of sloughing should also occur at a higher angle than observed in Fig. 7c, but this is obscured by the left atomizer boom. Comparison of the position of the strands between adjacent flights on the drum liner in the lower left corner of Fig. 7f shows that the strands land evenly distributed between the flights at position A and then slide into the corner formed by the flight and the liner at position B as the drum rotates. This motion is interpreted as follows: At the bottom of the blender drum, the 6:00 o'clock position, the centripetal and the gravitational forces acting on the strands are additive and the strands are pinned to the drum liner with no movement of the strands occurring. As the strands travel up the side of the drum, the gravitational force negates the frictional and centripetal forces holding the strands in place and the strands slide into the corner formed between the drum liner and the flight.

Increasing the rotation speed to 21 rpm increases the angle at which the strands begin to slough off the flights. From Figs. 7g and h strands can be seen sloughing off the first flight to the right of the left atomizer boom, but the boom again obscures the initial point of detachment. Comparing the distribution of strands between the first four flights beneath the left atomizer boom in Fig. 7h with those in Figs. 7b, 7d, and 7f shows that the strands were more evenly distributed between the flights at higher drum speeds. This is the result of the increased centrifugal force acting on the strands at the higher drum speeds, i.e., the drum must rotate further before the strands can slide over the drum liner and collect at the base of the flights.

Note also from Fig. 7h the collisions between the strands and right atomizer boom. In industrial blenders using liquid resins the atomizers are suspended from one or two booms making strand collisions with the boom or booms inevitable. The circular shape of the atomizer booms shown Fig. 7 is somewhat arbitrary. By tailoring the shape of the atomizer boom, e.g., a triangular cross section, one could better control the path of the strands as they collide with the boom and fall to the drum floor. For example, at low drum speeds, (Fig. 7a), the left atomizer boom could be redesigned to direct all of the strands to its right side, thus increasing the distance through which the strands fall and provide more opportunity for the stands to twirl and flip and collide with resin droplets. At higher drum speeds, (Fig. 7f), the right boom could be redesigned so that half of the strands are deflected off the left side of the boom and the other half off the right side. Since spinning disk atomizers spray resin in flat plane 360° from the axis of the atomizer mounts, this would permit the resin to be sprayed equally onto both strand streams.

Effect of free-fall distance on strand resination

The free-fall distance of the strands after detaching from a flight increased with rotation speed up to a point, and then decreased at higher rotation speeds. At 12.5 and 15.3 rpm, the strands fell a distance that was approximately equal to the diameter of the drum, whereas this distance decreased when the blender rotated at 18.4 rpm. At 21 rpm (Fig. 7h), the strands fell only about a third of the drum diameter. It is expected that the distance the strands fall after they detach from a flight will have a significant effect on the resination of strands. When strands are resting on the drum liner, resin can only be deposited on the top surface of the strands on top of the strand bundle. Once the strands slough and the bundle begins to spread, the strands twirl and flip and resin is more likely to be deposited onto both sides of the strands. The greater the free-fall distance, the more opportunity there is for both faces to come into contact with the resin droplets dispersed by the atomizers. It might be reason-

able to expect that the quantity of resin deposited on the strand surface increases linearly with free-fall distance. Furthermore, the spatial distribution of resin droplets on the strand surface is random and, given sufficient falling distance and number of falls, i.e., residence time, will tend towards a uniform distribution over the strand surface. The findings of McVey (1962), Lehmann (1965), Carroll and McVey (1962), Christensen and Robitschek (1974), and Kamke et al. (1996a) indicate that many small droplets dispersed over the strand surface produce stronger bonds between strands than fewer, but larger droplets dispersed over the same surface area. By extension, a board made from strands blended at 15.3 rpm may be more uniformly coated with resin and have better properties than one blended at 21 rpm due to the longer free fall distance of the strands. The blender shown in Fig. 7 has mounts for 16 atomizers and therefore the resin flow through each atomizer is much less than for a conventional blender containing one boom with 5 or 6 atomizers. Notwithstanding the more complex strand flow resulting from interference with two booms, one would expect this blender to coat strands with resin more uniformly than a blender with only 5 or 6 atomizers.

The highest rotation speed of 23.8 rpm (which is at the upper end of rotation speed range for a blender of this diameter), the strands took much longer to distribute themselves around the circumference of the blender than at lower speeds. Initially the strands were spread across only 6 to 8 flights, (Fig. 7i), compared with the 13 to 16 flights for the previous drum speed of 21 rpm, (Fig. 7g). This was primarily the result of the very small free-fall distance of the strands after they left the flights. From Fig. 7i, one can see that the strands had detached from the flights, but at this high speed the strands had significant horizontal velocity and they contacted the drum wall again very soon after leaving the previous flight. Eventually, after approximately 44 revolutions, the strands were distributed evenly around the circumference of the drum, as shown in Fig. 7j with very few strands detaching from any of the flights. At this speed, most of the strands simply slid back and forth between adjacent flights.

In Fig. 7j the five flights below the left atomizer boom are labeled A–E. The strands can be seen bundled against the right side of flights A, B, and C. Since the bundles between flights A and B and B and C appear to be the same size, one can conclude that no motion is occurring at these positions. Between flights C and D, the strand bundle begins to move away from flight D and towards flight C. Between flights D and E, the process has advanced further and the strand bundle has contacted the upper side of flight D. Examining the upper side of flight E, one can see that all of the strands have slid to that side. A similar positioning of strands was observed on the opposite side of the drum, but is partially obscured by the right boom. Strand bundles can be seen in contact with the bottom face of the flights above the right boom, labeled F and G. Examination of flight H below this boom shows that the strand bundles are now resting on the top face of that flight. Thus, although obscured by the boom, the strand bundle slid over the drum liner from the base of the higher flight to the base of the lower flight, shown schematically in Fig. 4c.

Effect of rotation speed on residence time

The average time a strand spends in the blender or "residence time" is of interest because it is thought that a longer residence time will lead to enhanced uniformity of resin distribution over strand surfaces. Travel times for strands from the feed chute to the edge of the field of view of the video camera for different rotation speeds are shown in Table 1; the corresponding number of drum revolutions is listed for comparative purposes. The times listed in Table 1 are the minimum times that strands spent in the blender with the majority of the strands taking more time to pass through the blender. It was not possible to directly measure residence time for the strands in the blender due to the difficulty of quantifying the rate at which strands passed through the exit chute. However, the effect of rotation speed on residence time could be estimated by comparing the time taken for the strands to travel from the feed chute to the edge of the field of view of the video camera. In terms of the theory developed

TABLE 1.   *The number of revolutions and the minimum time the strands remain in the blender at different drum speeds. Drum tilt angle is 3°.*

Drum speed (rpm)	No. of revolutions	Time (sec)
12.5	5.6	27
15.3	11.2	44
18.4	14.1	46
21.0	27.3	78
23.8	43.6	110

earlier, the rotation speeds in Table 1 are intermediate to high. From the table it is clear that strands move through the blender fastest at intermediate drum speeds, i.e., 12.5, 15.3, and 18.4 rpm, where the strand's free-fall distance is greatest and close to that of the drum diameter. At high speed strands remain in the blender longer because strands fall a shorter distance. Plotting the minimum residence time as a function of rotation speed, (Fig. 8) shows that residence time is proportional to rotations speed for a given tilt angle.

Although Fig. 8 suggests a longer residence time at high rotation speed, little twirling and flipping of the strands will occur because the free-fall distance of the strands is short. This leads to
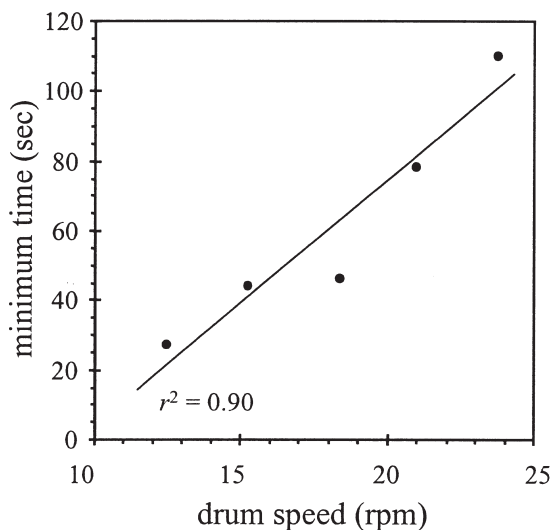

FIG. 8.   The time for the strands to travel from the infeed chute to the edge of the field of view of the video camera. Drum tilt angle is 3°.

highly variable resin coverage on strand surfaces and to boards with highly variable properties. To compensate for this, extra resin must be used, adding to production costs. Uniformity of resin coverage can be maximized by choosing a rotation speed that is high enough that the strands will slough off the flights many times, but not so high that the strands have insufficient time to twirl and flip and become coated with resin.

The capacities of commercial blenders using powdered and liquid PF-resins are listed in Table 2. The table shows that blenders using powdered resins have a throughput that is approximately 30% higher than that for a similar blender using liquid resins. Since the rotation speed for powdered blenders is lower than for liquid resins (Coil 2003a), the capacities listed in Table 2 are consistent with the earlier conclusions that rotation speed is directly proportional to residence time (Fig. 8). However, the tilt angle for blenders using powdered resin is less than for blenders using liquid resins, typically 2° for powders compared with 3 to 5° for liquids (Coil 2003b). Thus, the capacities listed in Table 2 are the result of the combined effect of rotation speed and tilt angle. Indeed, one might expect the throughput of industrial blenders with the same tilt angle as used for liquid resins to be even higher than those listed in Table 2 when processing a furnish containing powdered resin. Further research is needed to fully understand the interactions between tilt angle and rotation speed on strand residence time and uniformity of resination.

SUMMARY

The following conclusions and observations can be drawn from this investigation:

1. The incremental distance traveled parallel to the drum axis by strands with each revolution is inversely proportional to rotation speed.
2. The motion of the strands inside the blender is significantly affected by drum rotation speed. At low speed, strands are lifted up by flights and slough off when the angle formed between the edge of the strand bundle and the horizontal is larger than the angle of repose—these strands fall onto the adjacent flight. At intermediate speed, the angle of detachment is determined by an interplay between centrifugal forces and gravitational forces acting on a strand bundle—once sloughing has begun, strands continuously slough off from flights. As the drum speed increases, the furnish curtain moves across the width of the blender, in accord with the observations of Coil and Kasper (1984). At high speed, the centrifugal force keeps the strands pressed to the drum wall—these strands slide back and forth over the drum liner between adjacent flights.

TABLE 2. *Resination rates for powdered and liquid PF-resins for blenders with different drum sizes (data taken from datasheet "Blender Rated Capacity" Coil Manufacturing 2003).*

Drum dimensions diameter (ft)	length (ft)	Capacity for indicated resin type (1000 lbs/hr of oven dry OSB furnish)		Powdered/liquid ratio (–)
		powdered	liquid	
8	20	22	17	129
8	25	25	20	125
9	25	29	23	126
10	20	29	23	126
10	25	38.5	28.5	135
10	30	46.5	33	141
11	25	53	35.5	149
11	30	58	44	132
11	35	65	52	125
11	40	74	58	128
11	45	82	64	128

3. During free fall, the strands twirl and flip with the path taken by individual strands being quite chaotic, but the path of the center of gravity of the total strand mass is approximately parabolic.

4. As the strands fall, they spread and form a fan-shaped stream of strands.

5. The low volume of strands used in this study precludes observation of all possible types of strand tumbling that may occur in industrial blenders operating at full capacity for a given tilt angle.

6. The residence time of the strands in the blender is directly proportional to the rotation speed.

REFERENCES

BEATTIE, N. W. 1984. The Lignex spinning disc blender. *In* Proc. Washington State University Particleboard Symposium, Pullman, WA. 18:345–356.

CARROLL, M. N., AND D. McVEY. 1962. An analysis of resin efficiency in particleboard. Forest Prod. J. 12(7):305–310.

CHRISTENSEN R. L., AND P. ROBITSCHEK. 1974. Efficiency of resin-wood particle bonding. Forest Prod. J. 24(7):22–25.

COIL, G. K., AND J. B. KASPER. 1984. A liquid blending system developed by Mainland Manufacturing. *In* Proc. Washington State University Particleboard Symposium, Pullman, WA. 18:383–389.

COIL, M. Production Manager. Coil Manufacturing Limited, 8445-129A Street, Surrey, BC Canada, V3W 1A2. 2003a. Personal Communication. Telephone conversation with the author, 24 July.

———. Production Manager. Coil Manufacturing Limited, 8445-129A Street, Surrey, BC Canada, V3W 1A2. 2003b. Personal Communication. Telephone conversation with the author, 25 September.

CRAMOND, P., AND R. W. KNUDSON. 1984. Two approaches to blender design at CAE Machinery. *In* Proc. Washington State University Particleboard Symposium, Pullman, WA. 18:391–398.

DAVIS, E. W. 1919. Fine crushing in ball mills. Trans. Amer. Inst. Mining Metall. Eng. 61:250–296.

KAMKE, F. A., E. KULTIKOVA, AND C. A. LENTH. 1996a. OSB properties as affected by resin distribution. Pages 147–154 *in* Proc. Fourth International Panel and Engineered-Wood Technology Conference and Exposition.

———, C. A. LENTH, AND H. G. SAUNDERS. 1996b. Measurement of resin and wax distribution on wood flakes. Forest Prod. J. 46(6):63–68.

LEHMANN, W. F. 1965. Improved particleboard through better resin efficiency. Forest Prod. J. 15(4):155–161.

LIN, F. S. 1984. The globe blending system. *In* Proc. Washington State University Particleboard Symposium, Pullman, WA. 18:357–370.

SAUNDERS, H. G., AND F. A. KAMKE. 1996. Quantifying emulsified wax distribution on wood flakes. Forest Prod. J. 46(3):56–62.